

Termination of star formation by BH feedback in equal- and unequal-mass mergers of disk and elliptical galaxies

Peter H. Johansson^{1,*}, Thorsten Naab¹, Andreas Burkert¹

University Observatory Munich, Scheinerstr. 1, D-81679 Munich, Germany

Received 22 August 2008

Published online later

Key words galaxies: interaction– galaxies: active galaxies: evolution – galaxies: formation – methods: numerical

We present binary galaxy merger simulations of gas-rich disks (Sp-Sp), of early-type galaxies and disks (E-Sp, mixed mergers), and mergers of early-type galaxies (E-E, dry mergers) with varying mass ratios and different progenitor morphologies. The simulations include radiative cooling, star formation and black hole (BH) accretion and the associated feedback processes. We find for Sp-Sp mergers, that the peak star formation rate and BH accretion rate decrease and the growth timescales of the central black holes and newly formed stars increase with higher progenitor mass ratios. The termination of star formation by BH feedback in disk mergers is significantly less important for higher progenitor mass ratios (e.g. 3:1 and higher). In addition, the inclusion of BH feedback suppresses efficiently star formation in dry E-E mergers and mixed E-Sp mergers.

© 2006 WILEY-VCH Verlag GmbH & Co. KGaA, Weinheim

1 Introduction

Recent large-scale statistical galaxy surveys (e.g. the Sloan Digital Sky Survey (SDSS) and the two-degree Field (2df) survey) have revealed a robust bimodality in the observed galaxy population. Galaxies above a critical stellar mass of $M_{\text{crit}} \simeq 3 \times 10^{10} M_{\odot}$ are typically non-star forming red spheroidal systems with old stellar populations that predominantly live in dense environments, whereas galaxies below this critical mass are typically blue, star-forming disk galaxies that lie in the field (e.g. Bell et al. 2003; Kauffmann et al. 2003; Baldry et al. 2004; Balogh et al. 2004).

The observed bimodality can also be seen as a manifestation of cosmic downsizing, in which the most massive galaxies formed a significant proportion of their stars at high redshifts above $z \gtrsim 2$. The star formation is efficiently quenched in these systems by $z = 1$ as manifested in the observed population of extremely red non-starforming massive ellipticals (EROs, e.g. McCarthy 2004; Väisänen & Johansson 2004). The lower mass systems, on the contrary, have typically been forming stars throughout the whole cosmic epoch (e.g. Glazebrook et al. 2004; Juneau et al. 2005; Cimatti, Daddi, Renzini 2006).

The quenching mechanism responsible for the observed termination of star formation in massive galaxies at redshifts below $z \lesssim 2 - 3$ needs to be both energetic enough to trigger the quenching and long-lasting enough to maintain the quenching over a Hubble time. There exists several theoretical explanations for the quenching, including the feedback from AGNs (e.g. Bower et al. 2006; Croton et al. 2006), gaseous major mergers triggering star burst and/or quasar

activity (e.g. Naab, Jesseit, Burkert, 2006), quenching by shockheated gas above a critical halo mass (Dekel & Birnboim 2006; Birnboim, Dekel, Neistein 2007) and gravitational quenching by clumpy accretion (Naab et al. 2007; Dekel & Birnboim 2008).

In this paper we study the termination of star formation by black hole (BH) feedback in binary galaxy mergers. The study by Springel, Di Matteo, Hernquist (2005a) showed that BH feedback efficiently terminates star formation in equal-mass disk mergers. Here we confirm this result and expand the analysis to include unequal-mass disk mergers, mixed E-Sp mergers and dry E-E mergers. This paper is structured as follows. In §2 we briefly describe our simulation code and galaxy merger setup. We discuss the effect of varying the initial gas fractions, orbits, merger mass ratios and galaxy progenitors for terminating star formation in §3. Finally, we summarize and discuss our findings §4.

2 Simulations

We perform the simulations using the parallel TreeSPH-code GADGET-2 (Springel 2005) including star formation and the associated supernova feedback, where the multi-phase interstellar medium (Efstathiou 2000; Johansson & Efstathiou 2006) is modeled using the sub-resolution model developed by Springel & Hernquist (2003). We implemented a black hole feedback description similar to the Springel et al. (2005b) model into our version of the code. In this model the BH accretion rate is parameterized using a Bondi-Hoyle-Lyttleton description, with the maximum accretion rate limited to the Eddington rate. Finally, some fraction of the accreted rest mass energy is available as thermal

* Corresponding author: pjohan@usm.lmu.de

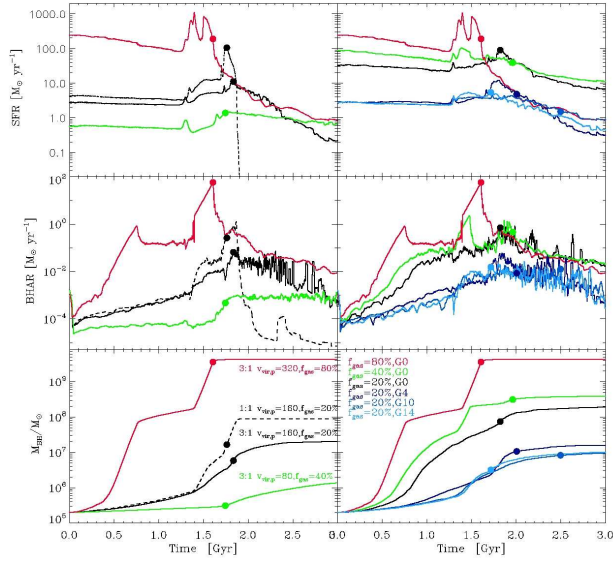


Fig. 1 The total star formation rate (top), the total black hole accretion rate (middle) and the evolution of the total black hole mass (bottom) as a function of time for three 3:1 (solid lines) and one 1:1 (dashed line) merger with initial gas mass fractions of 20% (black), 40% (green) and 80% (red) (*left panel*) and for three 3:1 mergers with varying initial gas mass fractions (black, green, red lines) and three 3:1 mergers with varying orbital and initial geometries for a fixed gas fraction (blue lines) (*right panel*). The filled circles indicate the time of merging of the BHs.

feedback energy that couples to the surrounding gas. Further details about the code implementation and parameter choices can be found in Johansson, Naab, Burkert (2008), J08 hereafter.

The disk galaxies are setup as described in J08, with Hernquist dark matter profiles populated by exponential disks with initial gas fractions ranging from 20% to 80%. All models contain initially a bulge with a third of the total disk mass. We also model mergers of early-type galaxies, where the early-type galaxies are setup initially using merger remnants of binary disk mergers (Naab & Burkert 2003). We set the primary galaxy models up with 20,000 gas and stellar disk particles, 10,000 bulge particles and 30,000 dark matter particles and scale the other models correspondingly. The gravitational softening lengths of gas, newly formed stars and the black hole particles are set to $\epsilon = 0.1h^{-1}\text{kpc}$ and the softening lengths of the disk, bulge and more massive dark matter particles are scaled with the square root of the particle masses resulting in $\epsilon = 0.2h^{-1}\text{kpc}$ for the bulge and disk particles and $\epsilon = 0.8h^{-1}\text{kpc}$ for the dark matter particles, respectively.

The galaxies are initially placed on parabolic orbits where the initial separation of the progenitors is set to the mean of the two galaxy virial radii and the pericentric distance to the mean of the two disk scale radii. All simulations presented in this paper were evolved for a total of $t = 3\text{ Gyr}$

using the local Altix 3700 Bx2 machine hosted at the University Observatory in Munich.

3 Results

In the left panel of Fig. 1 we plot the total star formation rates, BH accretion rates and the BH mass growth for three 3:1 mergers (solid lines) with 20% (black), 40% (green), 80% (red) initial gas mass fractions together with one 20% gas fraction 1:1 merger (dashed lines). The star formation is very efficiently terminated by the BH feedback in 1:1 mergers, compared to a generally much shallower decline in star formation for 3:1 mergers. In addition, the final BH masses are lower in 3:1 mergers typically by a factor of 2-5, but with a relatively large scatter depending on the progenitor masses and initial gas fractions.

In the right panel of Fig. 1 we show the results for three 3:1 mergers with varying initial gas mass fractions for a fixed orbit and initial disk geometry (black, green, red lines) and for three 3:1 mergers with varying initial orbits and orientations for a fixed gas mass fraction (blue lines). The initial gas fraction has a large effect on the height of the star formation and BH accretion peaks, with larger initial gas fractions producing higher values, as expected. This results also in relatively large differences in the final BH masses, with the $f_{\text{gas}} = 0.8$ simulations producing final BH masses that are larger by an order of magnitude compared to the $f_{\text{gas}} = 0.2$ runs. The variation of the orbit and initial geometry for a fixed gas mass fraction produces much smaller differences. The peaks of the star formation rates and BH accretion rates only vary within a factor of two with changing orbits and initial disk geometries.

In Fig. 2 we study the star formation and BH accretion histories for unequal-mass mergers with varying mass ratios. To this end we ran five mergers with mass ratios of 1:1, 2:1, 3:1, 4:1 and 6:1 on co-planar prograde orbits with initial gas mass fractions of 20%. As can be seen in Fig. 2 increasing the mass ratio of the merger systematically lowers the peak star formation rate and increases the duration of star formation activity after the merger. For the highest mass ratio merger the star formation rate is virtually constant throughout the simulation with only a mild peak during the first passage (see also di Matteo et al. 2007). The final BH masses are systematically lower for increasing mass ratio of the merger. Furthermore, the slope of the M_{BH} growth as a function of time becomes shallower with increasing merger mass ratio. There is also a systematic delay in the time of the BH merger with increasing mass ratio, as indicated by the filled circles in Fig. 2. For the lower mass ratio mergers the peak of the BH activity (the filled triangles in Fig. 2) typically occurs shortly after the merging of the BHs, whereas for the higher mass ratio mergers the peak of the BH activity is not directly related to the merging time of the BHs.

In Fig. 3 we study the duration of the BH accretion and star formation activity as a function of merger mass ratio.

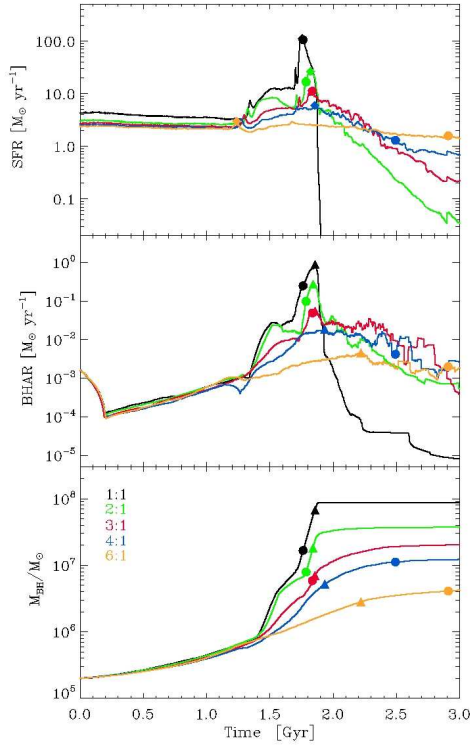


Fig. 2 The evolution of the star formation rates, black hole accretion rates and BH mass as a function of time for co-planar prograde 1:1 (black), 2:1 (green), 3:1 (red), 4:1 (blue) and 6:1 (orange) mergers. The filled circles indicate the time of the BH merger, the filled diamonds in the top panel and the filled triangles in the bottom two panels show the location of the maximum star formation and BH accretion peaks, respectively.

We define a half-mass growth time $\Delta T_{1/2}$ during which half of the final BH mass and half of the total stellar mass is formed respectively. In both cases $\Delta T_{1/2}$ is centered on the peak of the corresponding activity, the BH accretion on the maximum of the BH accretion rate (the triangles in Fig. 2) and the star formation rate on the peak of the SFR marked with diamonds in Fig. 2. The resulting half-mass timescales are shown in the bottom panel of Fig. 3. The $\Delta T_{1/2, \text{BH}}$ is strongly correlated with the mass ratio of the merger. For 1:1 and 2:1 mergers the growth of the M_{BH} is very concentrated in time, with half of the final BH mass growth occurring in less than 100 Myr. For the 3:1 and 4:1 mergers $\Delta T_{1/2, \text{BH}} \sim 0.5$ Gyr, with the 6:1 merger resulting in $\Delta T_{1/2, \text{BH}} \sim 1$ Gyr.

The corresponding stellar half-mass timescales $\Delta T_{1/2, \text{star}}$ (triangles in the bottom panel Fig. 3) also show a clear correlation with the mass ratio of the merger. In the 1:1 merger half of the final stellar mass is formed in a short major burst lasting about $\Delta T_{1/2, \text{star}} \sim 0.15$ Gyr. This value is comparable to the star formation timescale derived by Cox et al. (2008), who calculated a full width at half maximum of $\text{FWHM} \sim 0.1$ Gyr for the star formation peak of a typical

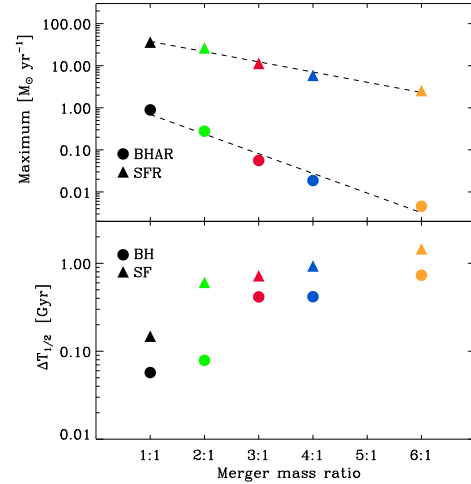


Fig. 3 The maximum BH accretion and star formation rates and timescales as a function of merger mass ratio. The bottom panel shows the half mass growth time of the BHs (circles) and the stellar mass (triangles) centered on the maximum BH accretion and star formation rates, respectively. The top panel shows the corresponding peak BH accretion (circles) and star formation rates (triangles) during the corresponding half mass growth time $\Delta T_{1/2}$.

1:1 merger. For higher mass-ratio mergers the resulting star formation timescales are $\Delta T_{1/2, \text{star}} \sim 0.7 - 1.0$ Gyr, with the highest mass-ratio merger having the longest timescale of $\Delta T_{1/2, \text{star}} \sim 1.5$ Gyr.

In the top panel of Fig. 3 we plot the corresponding maximum black hole accretion and star formation rates. By defining the variable q as the mass ratio between the primary and secondary component we can fit the logarithms of the peak BH accretion and star formation rates with the following linear relation

$$\log \text{Maximum} [\text{M}_{\odot} \text{yr}^{-1}] = a_0 + a_1 \times q, \quad (1)$$

where a_0 and a_1 are the inferred normalization and slope respectively. Both the maximum BH accretion rates and star formation rates are well fitted by Eq. 1 (dotted lines in Fig. 3) resulting in the following best fitting parameters respectively: $(a_{0, \text{BHAR}} = 0.31, a_{1, \text{BHAR}} = -0.47)$ ($a_{0, \text{SFR}} = 1.82, a_{1, \text{SFR}} = -0.24$). The ratio of the peak BH accretion rate to the peak star formation rate is thus of the order of $\dot{M}_{\text{BH, peak}} / \dot{M}_{\text{SF, peak}} \sim 10^{-2}$. On the other hand, the ratio of the mean BH accretion rate to the mean star formation averaged over the whole simulation is closer to $\dot{M}_{\text{BH, mean}} / \dot{M}_{\text{SF, mean}} \sim 10^{-3}$, with this ratio varying systematically between $\dot{M}_{\text{BH, mean}} / \dot{M}_{\text{SF, mean}} = 2 \cdot 10^{-3}$ (1:1 merger) and $\dot{M}_{\text{BH, mean}} / \dot{M}_{\text{SF, mean}} = 0.2 \cdot 10^{-3}$ (6:1 merger). Interestingly, recent observations of $z \sim 2$ galaxies by Daddi et al. 2007 also find indications of an universal ratio of $\dot{M}_{\text{BH}} / \dot{M}_{\text{SF}} \sim 10^{-3}$ and this is also expected from the observed $M_{\text{BH}} - M_*$ relation.

Finally, we analyse in Fig. 4 the star formation and BH accretion rates for a sample of four mixed E-Sp mergers (left panel) and four dry E-E mergers (right panel). The star formation rate of the mixed E-Sp mergers is lower than in Sp-Sp (Fig. 1) mergers, due to the lower amount of cold gas available for star formation. The disk progenitor contains $f_{\text{gas}} = 20\%$ of gas initially, whereas the early-type progenitors typically have an initial gas mass fraction of $f_{\text{gas}} \sim 5\%$, with typically only $\sim 1\%$ of this gas being cold and dense. After the merger of the E-Sp galaxies the star formation rate declines rapidly in all the merger remnants. We define a BH mass growth factor as $f_{\text{BH,insitu}} = \Delta M_{\text{BH,insitu}}/M_{\text{BH,final}}$, which gives the ratio of BH mass growth due to gas accretion during the simulation with respect to the final BH mass. Quantitatively, the fraction of the BH mass that accumulates by gas accretion during the mixed mergers is in the range of $f_{\text{BH,insitu}} \sim 20 - 50\%$, with typical mean values of $f_{\text{BH,insitu}} \sim 30\%$. For the E-E mergers the initial star formation rates are generally very low due to the low gas fractions of $f_{\text{gas}} \sim 1 - 5\%$. The initial gas fraction directly depends on the strength of the initial interaction that gave rise to the merger remnants used as progenitors for the E-E remergers. Increasing the masses of the progenitors and using more direct planar orbits produces more violent initial encounters, thus decreasing f_{gas} . The star formation is very effectively terminated shortly after the merging of the E-E progenitors on comparable timescales to 1:1 Sp-Sp mergers and thus more efficiently than in 3:1 Sp-Sp and mixed E-Sp mergers.

4 Conclusions

In this paper we have studied the termination of star formation in merger simulations including BH feedback. We find that the termination of star formation by BH feedback is significantly less important for unequal-mass disk mergers compared to equal-mass disk mergers. The timescale for star formation termination systematically increases with increasing progenitor mass ratios. Similarly, a systematic increase is seen in the half-mass growth timescales of the BHs, with this timescale varying from ~ 0.1 Gyr for equal-mass mergers to ~ 1 Gyr for 6:1 mergers. This systematic trend can be used as input in modeling BH accretion more realistically in semi-analytic galaxy formation models (e.g. Croton et al. 2006). For mass-ratios of 3:1 and higher mergers with BH feedback are unable to completely quench the star formation, with the merger remnants showing star formation rates roughly on the pre-merger level even 1 Gyr after completion of the merger. In addition, the star formation is efficiently terminated in mixed E-Sp and dry E-E mergers due to the presence of the fully grown super-massive BHs in the early-type progenitors.

Acknowledgements. The numerical simulations were performed on the local SGI-Altix 3700 Bx2, which was partly funded by the Cluster of Excellence: "Origin and Structure of the Universe".

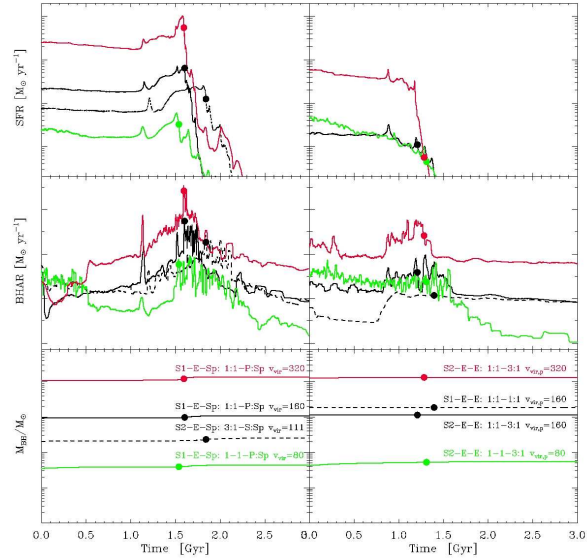


Fig. 4 The total star formation rate (top), the total black hole accretion rate (middle) and the evolution of the total black hole mass (bottom) as a function of time for four E-Sp mixed mergers (*left panel*) and four E-E remergers (*right panel*). The gas disks have initially $f_{\text{gas}} = 20\%$ and the virial velocities as indicated in the Figure. The filled circles indicate the time of merging of the BHs.

References

- Baldry, I. K. et al.: 2004, *ApJ*, 600, 681
 Balogh, M. L. et al.: 2004, *ApJ*, 615, 101
 Bell, E. F., et al.: 2003, *ApJS*, 149, 289
 Birnboim, Y., Dekel, A., Neistein, E., 2007, *MNRAS*, 380, 339
 Bower, R. G et al.: 2006, *MNRAS*, 370, 645
 Cimatti, A., Daddi, E., Renzini, A.: 2006, *A&A*, 453, 29
 Croton, D. J., et al.: 2006, *MNRAS*, 365, 11
 Cox, T.J. et al., 2008, 384, 386
 Daddi, E. et al.: 2007, *ApJ*, 670, 156
 Dekel, A. & Birnboim, Y.: 2006, *MNRAS*, 368, 2
 Dekel, A. & Birnboim, Y.: 2008, *MNRAS*, 383, 119
 di Matteo, P. et al.: 2007, *A&A*, 468, 61
 Efstathiou, G: 2000, *MNRAS*, 317, 697
 Glazebrook, K. et al.: 2004, *Nature*, 430, 181
 Johansson, P. H. & Efstathiou, G., 2006, *MNRAS*, 371, 1519
 Johansson, P. H., Naab, T., Burkert, A., 2008, *ApJ* in press, arXiv:0802.0210
 Juneau, S. et al: 2005, *ApJ*, 619, 135
 Kauffmann, G. et al.: 2003, *MNRAS*, 341, 33
 McCarthy, P. J.: 2004, *ARA&A*, 42, 427
 Naab, T. & Burkert, A.: 2003, *ApJ*, 597, 893
 Naab, T., Jesseit, R., Burkert, A.: 2006, *MNRAS*, 327, 839
 Naab, T., Johansson, P. H., Ostriker, J. P, Efstathiou, G.: 2007, *ApJ*, 658, 710
 Springel, V.: 2005, *MNRAS*, 364, 1105
 Springel, V. & Hernquist, L.: 2003, 339, 289
 Springel, V., Di Matteo, T., Hernquist, L.: 2005a, *ApJ*, 620, 79
 Springel, V., Di Matteo, T., Hernquist, L.: 2005b, *MNRAS*, 361, 776
 Väisänen, P. & Johansson, P. H.: 2004, *A&A*, 421, 821